



LAWRENCE
LIVERMORE
NATIONAL
LABORATORY

Latent Image Volumetric Additive Manufacturing

C. M. Rackson, J. T. Toombs, M. P. De Beer, C. C. Krikorian, M. Shusteff, H. K. Taylor, R. R. McLeod

October 21, 2021

Optics Letters

Disclaimer

This document was prepared as an account of work sponsored by an agency of the United States government. Neither the United States government nor Lawrence Livermore National Security, LLC, nor any of their employees makes any warranty, expressed or implied, or assumes any legal liability or responsibility for the accuracy, completeness, or usefulness of any information, apparatus, product, or process disclosed, or represents that its use would not infringe privately owned rights. Reference herein to any specific commercial product, process, or service by trade name, trademark, manufacturer, or otherwise does not necessarily constitute or imply its endorsement, recommendation, or favoring by the United States government or Lawrence Livermore National Security, LLC. The views and opinions of authors expressed herein do not necessarily state or reflect those of the United States government or Lawrence Livermore National Security, LLC, and shall not be used for advertising or product endorsement purposes.

Latent Image Volumetric Additive Manufacturing

CHARLES M. RACKSON^{1*}, JOSEPH T. TOOMBS³, MARTIN P. DE BEER⁴, CAITLYN C. COOK⁴, MAXIM SHUSTEFF⁴, HAYDEN K. TAYLOR³, ROBERT R. MCLEOD^{1,2}

¹Department of Electrical, Computer, and Energy Engineering, University of Colorado, Boulder, CO 80309, USA.

²Materials Science & Engineering, University of Colorado, Boulder, CO 80303, USA.

³Department of Mechanical Engineering, University of California, Berkeley, Berkeley, CA 94720, USA.

⁴Lawrence Livermore National Laboratory, Livermore, CA 94550, USA.

*Corresponding author: charles.rackson@colorado.edu

Received XX Month XXXX; revised XX Month, XXXX; accepted XX Month XXXX; posted XX Month XXXX (Doc. ID XXXXX); published XX Month X

Volumetric additive manufacturing (VAM) enables rapid printing into a wide range of materials, offering significant advantages over other printing technologies, with a lack of inherent layering of particular note. However, VAM suffers from striations, similar in appearance to layers, and similarly limiting applications due to mechanical and refractive index inhomogeneity, surface roughness, etc. We hypothesize that these striations are caused by a self-written waveguide effect, driven by the gelation material nonlinearity upon which VAM relies, and that they are not a direct recording of non-uniform patterning beams. We demonstrate a simple and effective method of mitigating striations via a uniform optical exposure added to the end of any VAM printing process. We show this step to additionally shorten the period from initial gelation to print completion, mitigating the problem of partially gelled parts sinking before print completion, and expanding the range of resins printable in any VAM printer.

1. INTRODUCTION

Multi-step additive manufacturing (AM) is being pursued for a wide range of applications [1] such as: printing optics [2–4], microfluidics [5–7], composites with overprinting [8,9], regenerative medicine [10–13], etc. However, inherent to multi-step AM are layering effects [14–16] which limit the performance and applications of printed parts via mechanical inhomogeneity and anisotropy, non-uniform refractive index of printed optics, and cosmetic imperfection.

Volumetric Additive Manufacturing (VAM) prints into a volume of photosensitive resin in a single lithographic step, and is thus free of inherent layering effects. After tens to hundreds of seconds of optical exposures the desired geometry gels and is removed from the remaining liquid resin. Fundamental to this process is a material nonlinearity – a gelation threshold – which enables delivery of optical dose for selective gelation of the desired print volume without unwanted gelation of the surrounding resin. This approach has multiple advantages over multi-step AM. Non-contiguous prints become possible; the lack of material movement during printing

removes resin viscosity constraints, thus increasing the range of accessible material properties; print times are dramatically reduced and layering is fundamentally absent from the printing process. However, VAM prints [17–21] suffer from large striations – similar in appearance to layering, and on the order of print feature size – impacting the homogeneity and shape-accuracy of printed parts, and presenting a significant cosmetic defect.

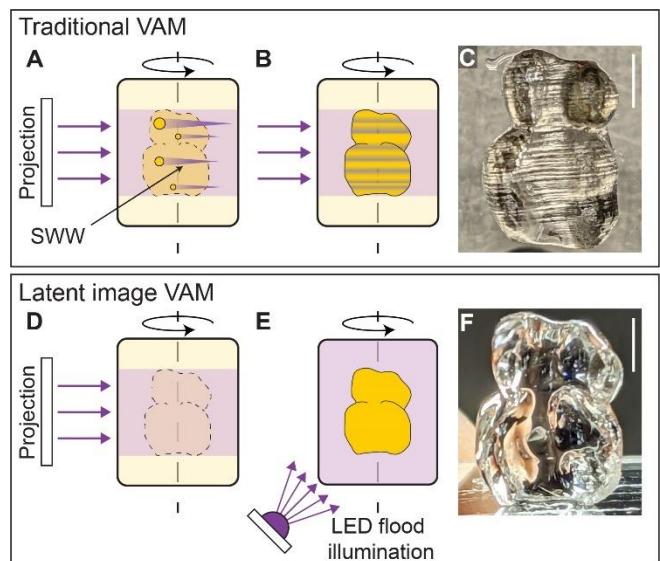


Figure 1. **A–B:** A conventional VAM print process. **C:** Resultant dental aligner print exhibiting typical striations. As detailed in Section 2, initial local gelation causes focusing, leading to a self-written-waveguide (SWW) effect, manifesting as striations (scale bars: 3 mm). **D–E:** The latent-image process proposed here. **D:** Patterning is stopped just before gelation occurs, leaving a 3D latent image of polymer conversion that is higher in the desired print region than in the surrounding resin. **E:** The latent image is developed across the gelation threshold via diffuse, uniform LED illumination, driving only the desired region to gelation. **F:** The resultant print exhibits dramatically reduced striations, with a smooth surface and improved refractive index homogeneity.

In this paper, we examine the source of striations in VAM, and discuss the hypothesis that the material nonlinearity upon which VAM relies also drives striations via a *self-writing waveguide* (SWW) effect. We present a simple and effective method of dramatically reducing striations (Fig. 1F) via the addition of a uniform optical exposure applied to the entire volume of resin at the end of a print. Here, VAM patterning starts as usual, steadily increasing polymer conversion in the desired print-regions, but not past the gelation threshold as is typical. Instead, the patterning is stopped just before this material nonlinearity is reached (see Supplemental Information for further timing details), then a flood exposure develops the resultant latent image to gelation (Fig. 1D-E). We discuss how the technique affects the system tolerances required to maintain theoretically perfect print fidelity. We show that the method has the additional advantage of drastically reducing the *gelation period* (GP) of a print, defined here as the time between the first appearance of any gelation and the print completion. This mitigates the problem of partial-print sinking in low power or low viscosity prints, thus further expanding resin options and increasing the efficacy of low-cost VAM printers. We conclude by discussing future work and potential improvements to the method.

2. STRIATIONS IN VAM

Striations are a ubiquitous problem in the field of VAM. A variety of volumetric printers applied to a wide range of materials suffer from large striations on the order of feature size [17–21]. Such striations not only degrade print-shape accuracy, but any non-uniformities in polymer conversion can manifest as inhomogeneity or anisotropy of modulus, or as unwanted refractive index variability. Thus, although VAM is free from layering, it is not free from layer-like effects. Examples of typical VAM striations are shown in Fig. 2. Here, we discuss the hypothesis that striations are caused by a SWW effect, driven by the material nonlinearity upon which VAM fundamentally relies, and that striations are not caused by the direct recording of non-uniform patterning beams.

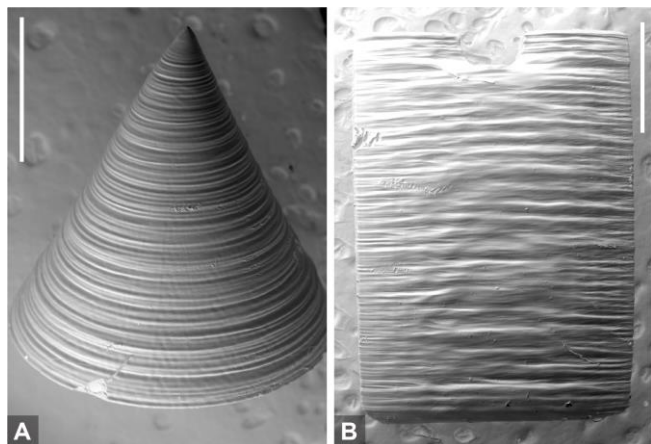


Figure 2. Scanning electron microscopy (SEM) scans of typical striations in conventional VAM prints. **A:** A cone printed with the axis of rotation aligned with the central axis of the cone. A roughly 60 μm striation pitch was measured both near the tip of cone, where the focused beam size was measured to be 11 μm , and near the base of the cone, where the beam size was 23 μm . A single projector pixel was measured to have a focused size of 6 and 18 μm at the center and at the edge of the print,

respectively. **B:** A slab print – the same as in Fig. 3A, B, F, G – exhibiting irregular striations. Scale bars: 1 mm. See Supplemental Information for further print details.

The strongest evidence that VAM striations are not a direct recording of writing beams is that the latent cure method detailed in this paper effectively suppresses striations. With this method, typically about 90% of the printing dose is delivered by patterned writing beams before gelation, and then the final 10% of dose is delivered by a uniform exposure. If striations were simply a direct recording of non-uniform beams, we would expect to see them develop along with the rest of the part during latent cure. Striation visibility would likely be reduced by the uniform exposure, but only by a small amount. Instead, we observe a nearly complete elimination of striations, suggesting a fundamental difference between using highly directional patterned illumination and an angularly-diffuse flood exposure to cross the gelation threshold.

We hypothesize that striations in VAM are due to a SWW effect. This effect is well-known to occur in many photopolymer exposure systems [22], and has been employed to manufacture waveguides [23–27]. Here, as light gels a small region of material, the refractive index increase of this phase change acts as a lens, concentrating the light to the resin just beyond it. The increased intensity causes this next region to also gel more quickly than the surrounding resin. This continues, with each new region of gelation building upon the growing waveguide, until a long waveguide – a striation of increased index – extends through the print region. The properties of SWWs are complex and have been extensively studied in the literature. Notably, depending on material index-change dynamics and on the intensity profile of writing beams, SWWs can form with variable widths, not matching the size of the writing beams. SWWs can be unstable in their propagation direction, and filamentation can also occur, with stochastic splitting and merging behavior [27,28].

The SWW effect is most pronounced when the refractive index of the material changes most quickly with conversion; that is, during the gelation phase change. The much smaller index change of pre-gelation conversion also produces SWWs, as perhaps seen in the liquid resin surrounding the prints in Fig. 3A, F, D. However, their impact appears to be negligible, as evidenced by the striation-free prints presented in this paper. Thus, prominent print striations would be expected only when highly directional illumination, such as VAM patterning beams, are incident on a material near the start of gelation. As detailed in the next section, avoiding directional illumination as the material gels dramatically reduces striations in VAM prints.

2. LATENT CURE METHOD

Here we describe a simple, effective, and inexpensive method of avoiding striations in any VAM printing process by using diffuse light instead of highly directly patterning beams to cross the material nonlinearity. In this method, a print starts as usual with patterned illumination locally increasing polymer conversion in the resin. Just before gelation is reached, the writing is stopped, leaving a latent image of the desired print in the form of higher polymer conversion and oxygen depletion for the desired in-part regions than the surrounding out-of-part regions. Then, an LED with a diffuser applies a low-spatial-coherence, uniform exposure to the entire volume of resin such that the light is incident from a wide range of angles (Fig. 1E). This develops the latent image into a gelled

part, and the flood illumination is ceased before unwanted gelation occurs in the surrounding out-of-part regions, thus preserving

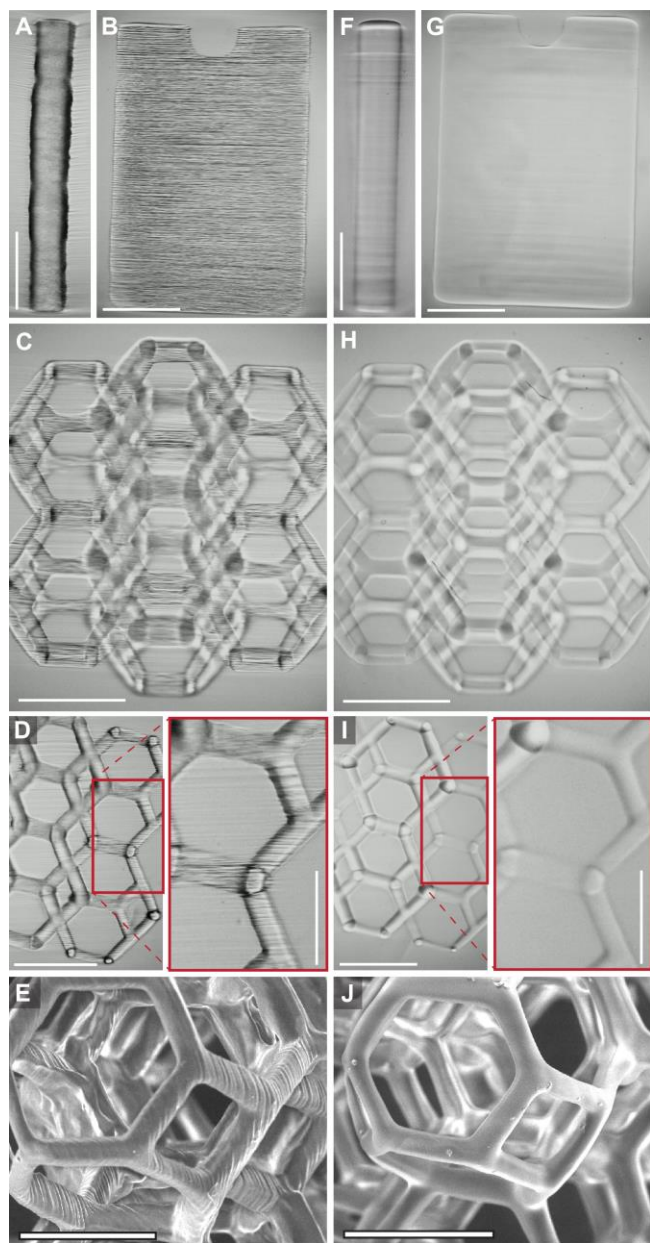


Figure 3. Striation mitigation by the latent cure method proposed in this paper. **A–D**: Shadowgrams and **E**: SEM scan of conventional VAM prints of a slab, mesh, and tilted mesh showing striations on the order of feature size upon completion. **F–J**: The same geometries printed using the latent cure method. Striations are largely eliminated, both in surface roughness (**J**), and in refractive index uniformity shown via shadowgrams of prints still immersed in resin (**F–J**). **A–B** and **F–G** illustrate the improved shape fidelity yielded by the method. Scale bars: 1 mm for **A–J**, with 500 μm for zooms. The shadowgrams were captured with the basic collimated LED shadowgraph setup described in [29].

selective gelation. With this method, patterning illumination is ideally stopped just before any gelation occurs. In practice, stopping the print slightly earlier or slightly later – at the first sign of gelation

on a shadowgram - still produces good results. See the Supplemental Information for further exposure and timing details. The resultant print exhibits dramatically reduced striations, as shown in Figures 1 and 3 which compare the current and proposed VAM processes. The shadowgrams in Fig 3A-H, which highlight even small refractive index changes [29,30] suggest improved uniformity, although measurements without the surrounding resin in place would be more conclusive. Lastly, surface striation effects are eliminated, as shown via SEM scans in Fig. 3E and 3K. The uniform exposure decreases the dose-contrast between in-part and out-of-part regions, reducing system error tolerances, but only by a small fraction equal to the in-part dose range [31] of the tomographic reconstruction - about 10% for typical prints. Thus, a theoretically perfect VAM print – one free of missing or unwanted gelled voxels – will remain so upon latent cure (see the Supplemental Information for further details). The latent cure method appears to only require an LED and diffuser for good results; however, the non-directionality of the latent cure could be improved via multiple light sources, an integrating sphere around the print, or any other modification to increase the range of input angles over which the flood exposure is delivered.

4. LATENT CURE TO AVOID PARTIAL-PRINT SINKING

The latent cure step also serves as an opportunity to apply high intensity optical exposure during the GP of a print. This can dramatically shorten the GP, ameliorating the distortion of a print due to partial part sinking during printing [18].

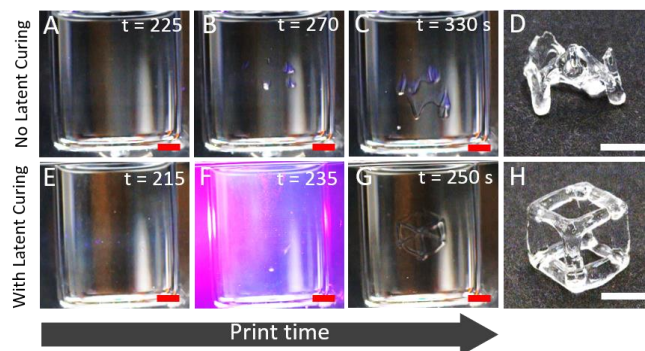


Figure 4. Latent cure as a method of speeding the GP in a low power VAM print. **A–D**: Conventional VAM process, suffering from low print power and low viscosity resin. The partially-gelled regions sink before the part is complete. **D**: Severely distorted final part. **E–H**: VAM print with latent cure used to quickly develop the entire print through its GP before significant sinking occurs. Even though the patterning process and viscosity were unchanged from **A–D**, the rapid gelation via latent cure results in, **H**: a significantly improved print. See **Visualization 1** for videos of the prints. The GP could be easily further shortened by increasing the power of the latent exposure. In this case, a GP of only a few seconds was difficult to control, so the latent-cure power was reduced so that gelation could be easily observed, and the latent exposure stopped before unwanted gelation.

This effect occurs when the polymerization rate is slow relative to the settling velocity of the gelled material, as is the case for systems with low print power, low viscosity resins, or large change in the density upon gelation [32,33]. An inexpensive latent cure source,

free of the etendue requirements that practically limit patterned print power [18], can be added to any VAM system to expand the range of materials that it can accurately print. This could allow low-power VAM printers to use resins previously only accessible by costly, high-power systems, just as it could allow state of the art, high-power printers access to a new range of resins. Figure 4 shows an example of how latent cure enables printing in a low viscosity (<1 Pa.s) resin that would otherwise be untenable, given printer-power.

5. CONCLUSIONS

Like the layering effects that limit the applications of typical 3D printing methods, striations in VAM can cause non-uniformity in modulus and refractive index, and degrade print-surface accuracy. We discussed the hypothesis that striations are not simply recorded writing beams, and are instead caused by a SWW effect [22–25,27], driven by the material nonlinearity upon which VAM fundamentally relies. This effect can be avoided by adding a diffuse latent-cure step. We showed the improved uniformity yielded by this method, we discussed how the resultant reduction in system error tolerances is small, and how theoretically-perfect [31] printing is maintained by the method. We demonstrated the latent cure step as method of quickly delivering optical power during the GP of a print, mitigating the problem of partial-print sinking that plagues low-power VAM printers, or resins with a particularly low viscosity or high degree of densification upon gelation. Future work could improve timing control of the latent cure, allowing for sub-second GPs. Lastly, the non-directionality of the latent cure could be improved by an array of lamps, by a surrounding integrating sphere, etc., improving the uniformity of the method, and minimizing the SWW effect.

Funding.

This work was partly performed under the auspices of the U.S. Department of Energy by Lawrence Livermore National Laboratory under Contract DE-AC52-07NA27344. LLNL-JRNL-828179.

Supported by The National Science Foundation under Cooperative Agreement No. EEC-1160494. Supported by the LLNL Laboratory-Directed Research & Development (LDRD) program.

Disclosures.

H. Taylor and M. Shusteff hold U.S. patent 10,647,061 B2 relating to computed axial lithography, also known as tomographic VAM. C. Rackson has filed provisional patent No. 63/231,395 regarding latent image VAM. C. Rackson and R. McLeod have filed provisional patent No 63/181,645 regarding computational and other methods for VAM.

Data availability. Data available upon request.

See Supplement 1 for supporting content.

REFERENCES

- C. Schubert, M. C. van Langeveld, and L. A. Donoso, *British Journal of Ophthalmology* **98**, 159–161 (2014).
- D. T. Nguyen, C. Meyers, T. D. Yee, N. A. Dudukovic, J. F. Destino, C. Zhu, E. B. Duoss, T. F. Baumann, T. Suratwala, J. E. Smay, and R. Dylla-Spears, *Advanced Materials* **29**, 1701181 (2017).
- T. Gissibl, S. Thiele, A. Herkommer, and H. Giessen, *Nature Photonics* **10**, 554–560 (2016).
- S. Thiele, K. Arzenbacher, T. Gissibl, H. Giessen, and A. M. Herkommer, *Science Advances* **3**, e1602655 (2017).
- H. Gong, B. P. Bickham, A. T. Woolley, and G. P. Nordin, *Lab Chip* **17**, 2899–2909 (2017).
- S. Waheed, J. M. Cabot, N. P. Macdonald, T. Lewis, R. M. Guijt, B. Paull, and M. C. Breadmore, *Lab on a Chip* **16**, 1993–2013 (2016).
- R. Amin, S. Knowlton, A. Hart, B. Yenilmez, F. Ghaderinezhad, S. Katebifar, M. Messina, A. Khademhosseini, and S. Tasoglu, *Biofabrication* **8**, 022001 (2016).
- C. Jianu, G. Lamanna, and C. G. Opran, *Materials Science Forum; Pfaffikon* **957**, 267–276 (2019).
- M. N. Jahangir, J. Cleeman, H.-J. Hwang, and R. Malhotra, *Additive Manufacturing* **30**, 100886 (2019).
- E. S. Bishop, S. Mostafa, M. Pakvasa, H. H. Luu, M. J. Lee, J. M. Wolf, G. A. Ameer, T.-C. He, and R. R. Reid, *Genes & Diseases* **4**, 185–195 (2017).
- N. Noor, A. Shapira, R. Edri, I. Gal, L. Wertheim, and T. Dvir, *Advanced Science* **6**, 1900344 (2019).
- M. Randazzo, J. M. Pisapia, N. Singh, and J. P. Thawani, *Surg Neurol Int* **7**, S801–S809 (2016).
- L. A. Hockaday, K. H. Kang, N. W. Colangelo, P. Y. C. Cheung, B. Duan, E. Malone, J. Wu, L. N. Girardi, L. J. Bonassar, H. Lipson, C. C. Chu, and J. T. Butcher, *Biofabrication* **4**, 035005 (2012).
- N. Alharbi, R. Osman, and D. Wismeijer, *The Journal of Prosthetic Dentistry* **115**, 760–767 (2016).
- K. Kowsari, B. Zhang, S. Panjwani, Z. Chen, H. Hingorani, S. Akbari, N. X. Fang, and Q. Ge, *Additive Manufacturing* **24**, 627–638 (2018).
- A. V. Shembekar, Y. J. Yoon, A. Kanyuck, and S. K. Gupta, in *(American Society of Mechanical Engineers Digital Collection, 2018)*.
- B. E. Kelly, I. Bhattacharya, H. Heidari, M. Shusteff, C. M. Spadaccini, and H. K. Taylor, *Science* **363**, 1075–1079 (2019).
- D. Loterie, P. Delrot, and C. Moser, *Nat Commun* **11**, 852 (2020).
- C. C. Cook, E. J. Fong, J. J. Schwartz, D. H. Porcincula, A. C. Kaczmarek, J. S. Oakdale, B. D. Moran, K. M. Champley, C. M. Rackson, A. Muralidharan, R. R. McLeod, and M. Shusteff, *Advanced Materials*, 2003376 (2020).
- I. Bhattacharya, J. Toombs, and H. Taylor, *Additive Manufacturing* **47**, 102299 (2021).
- A. Orth, K. L. Sampson, K. Ting, K. Ting, J. Boisvert, and C. Paquet, *Opt. Express*, OE **29**, 11037–11054 (2021).
- R. Malallah, H. Li, D. P. Kelly, J. J. Healy, and J. T. Sheridan, *Polymers* **9**, 337 (2017).
- M. Kagami, T. Yamashita, and H. Ito, *Appl. Phys. Lett.* **79**, 1079–1081 (2001).
- A. S. Kewitsch and A. Yariv, *Opt. Lett.*, OL **21**, 24–26 (1996).
- R. Malallah, D. Cassidy, I. Muniraj, J. P. Ryle, J. J. Healy, and J. T. Sheridan, *Appl. Opt.* **57**, E80 (2018).
- A. J. Jacobsen, W. Barvosa-Carter, and S. Nutt, *Advanced Materials* **19**, 3892–3896 (2007).
- R. Malallah, H. Li, I. Muniraj, D. Cassidy, N. Al-Attar, J. J. Healy, and J. T. Sheridan, *J. Opt. Soc. Am. B* **35**, 2046 (2018).
- N. Hô, B. Bourliaguet, J. M. Laniel, R. Vallée, and A. Villeneuve, *Nonlinear Guided Waves and Their Applications* (OSA, 2001), p. WC8.
- J. Toombs, M. Luitz, C. Cook, S. Jenne, C. C. Li, B. Rapp, F. Kotz-Helmer, and H. Taylor, arXiv:2110.01651 [physics] (2021).
- C. Chung Li, J. Toombs, and H. Taylor, *Symposium on Computational Fabrication, SCF '20* (Association for Computing Machinery, 2020), pp. 1–7.
- C. M. Rackson, K. M. Champley, J. T. Toombs, E. J. Fong, V. Bansal, H. K. Taylor, M. Shusteff, and R. R. McLeod, *Additive Manufacturing* **48**, 102367 (2021).
- Y. Jian, Y. He, L. Zhao, A. Kowalczyk, W. Yang, and J. Nie, *Advances in Polymer Technology* **32**, (2013).
- D. L. Kurdikar and N. A. Peppas, *Polymer* **36**, 2249–2255 (1995).

REFERENCES WITH TITLES (FOR REVIEW)

1. C. Schubert, M. C. van Langeveld, and L. A. Donoso, "Innovations in 3D printing: a 3D overview from optics to organs," *British Journal of Ophthalmology* **98**, 159–161 (2014).
2. D. T. Nguyen, C. Meyers, T. D. Yee, N. A. Dudukovic, J. F. Destino, C. Zhu, E. B. Duoss, T. F. Baumann, T. Suratwala, J. E. Smay, and R. Dylla-Spears, "3D-Printed Transparent Glass," *Advanced Materials* **29**, 1701181 (2017).
3. T. Gissibl, S. Thiele, A. Herkommer, and H. Giessen, "Two-photon direct laser writing of ultracompact multi-lens objectives," *Nature Photonics* **10**, 554–560 (2016).
4. S. Thiele, K. Arzenbacher, T. Gissibl, H. Giessen, and A. M. Herkommer, "3D-printed eagle eye: Compound microlens system for foveated imaging," *Science Advances* **3**, e1602655 (2017).
5. H. Gong, B. P. Bickham, A. T. Woolley, and G. P. Nordin, "Custom 3D printer and resin for 18 μm \times 20 μm microfluidic flow channels," *Lab Chip* **17**, 2899–2909 (2017).
6. S. Waheed, J. M. Cabot, N. P. Macdonald, T. Lewis, R. M. Guijt, B. Paull, and M. C. Breadmore, "3D printed microfluidic devices: enablers and barriers," *Lab on a Chip* **16**, 1993–2013 (2016).
7. R. Amin, S. Knowlton, A. Hart, B. Yenilmez, F. Ghaderinezhad, S. Katebifar, M. Messina, A. Khademhosseini, and S. Tasoglu, "3D-printed microfluidic devices," *Biofabrication* **8**, 022001 (2016).
8. C. Jianu, G. Lamanna, and C. G. Opran, "Research Regarding Embedded Systems of Robotic Technology for Manufacturing of Hybrid Polymeric Composite Products," *Materials Science Forum; Pfaffikon* **957**, 267–276 (2019).
9. M. N. Jahangir, J. Cleeman, H.-J. Hwang, and R. Malhotra, "Towards out-of-chamber damage-free fabrication of highly conductive nanoparticle-based circuits inside 3D printed thermally sensitive polymers," *Additive Manufacturing* **30**, 100886 (2019).
10. E. S. Bishop, S. Mostafa, M. Pakvasa, H. H. Luu, M. J. Lee, J. M. Wolf, G. A. Ameer, T.-C. He, and R. R. Reid, "3-D bioprinting technologies in tissue engineering and regenerative medicine: Current and future trends," *Genes & Diseases* **4**, 185–195 (2017).
11. N. Noor, A. Shapira, R. Edri, I. Gal, L. Wertheim, and T. Dvir, "3D Printing of Personalized Thick and Perfusable Cardiac Patches and Hearts," *Advanced Science* **6**, 1900344 (2019).
12. M. Randazzo, J. M. Pisapia, N. Singh, and J. P. Thawani, "3D printing in neurosurgery: A systematic review," *Surg Neurol Int* **7**, S801–S809 (2016).
13. L. A. Hockaday, K. H. Kang, N. W. Colangelo, P. Y. C. Cheung, B. Duan, E. Malone, J. Wu, L. N. Girardi, L. J. Bonassar, H. Lipson, C. C. Chu, and J. T. Butcher, "Rapid 3D printing of anatomically accurate and mechanically heterogeneous aortic valve hydrogel scaffolds," *Biofabrication* **4**, 035005 (2012).
14. N. Alharbi, R. Osman, and D. Wismeijer, "Effects of build direction on the mechanical properties of 3D-printed complete coverage interim dental restorations," *The Journal of Prosthetic Dentistry* **115**, 760–767 (2016).
15. K. Kowsari, B. Zhang, S. Panjwani, Z. Chen, H. Hingorani, S. Akbari, N. X. Fang, and Q. Ge, "Photopolymer formulation to minimize feature size, surface roughness, and stair-stepping in digital light processing-based three-dimensional printing," *Additive Manufacturing* **24**, 627–638 (2018).
16. A. V. Shembekar, Y. J. Yoon, A. Kanyuck, and S. K. Gupta, "Trajectory Planning for Conformal 3D Printing Using Non-Planar Layers," in (American Society of Mechanical Engineers Digital Collection, 2018).
17. B. E. Kelly, I. Bhattacharya, H. Heidari, M. Shusteff, C. M. Spadaccini, and H. K. Taylor, "Volumetric additive manufacturing via tomographic reconstruction," *Science* **363**, 1075–1079 (2019).
18. D. Loterie, P. Delrot, and C. Moser, "High-resolution tomographic volumetric additive manufacturing," *Nat Commun* **11**, 852 (2020).
19. C. C. Cook, E. J. Fong, J. J. Schwartz, D. H. Porcincula, A. C. Kaczmarek, J. S. Oakdale, B. D. Moran, K. M. Champley, C. M. Rackson, A. Muralidharan, R. R. McLeod, and M. Shusteff, "Highly Tunable Thiol-Ene Photoresins for Volumetric Additive Manufacturing," *Advanced Materials*, 2003376 (2020).
20. I. Bhattacharya, J. Toombs, and H. Taylor, "High fidelity volumetric additive manufacturing," *Additive Manufacturing* **47**, 102299 (2021).
21. A. Orth, K. L. Sampson, K. Ting, K. Ting, J. Boisvert, and C. Paquet, "Correcting ray distortion in tomographic additive manufacturing," *Opt. Express, OE* **29**, 11037–11054 (2021).
22. R. Malallah, H. Li, D. P. Kelly, J. J. Healy, and J. T. Sheridan, "A Review of Hologram Storage and Self-Written Waveguides Formation in Photopolymer Media," *Polymers* **9**, 337 (2017).
23. M. Kagami, T. Yamashita, and H. Ito, "Light-induced self-written three-dimensional optical waveguide," *Appl. Phys. Lett.* **79**, 1079–1081 (2001).
24. A. S. Kewitsch and A. Yariv, "Self-focusing and self-trapping of optical beams upon photopolymerization," *Opt. Lett., OL* **21**, 24–26 (1996).
25. R. Malallah, D. Cassidy, I. Muniraj, J. P. Ryle, J. J. Healy, and J. T. Sheridan, "Self-written waveguides in photopolymer," *Appl. Opt.* **57**, E80 (2018).
26. A. J. Jacobsen, W. Barvosa-Carter, and S. Nutt, "Micro-scale Truss Structures formed from Self-Propagating Photopolymer Waveguides," *Advanced Materials* **19**, 3892–3896 (2007).
27. R. Malallah, H. Li, I. Muniraj, D. Cassidy, N. Al-Attar, J. J. Healy, and J. T. Sheridan, "Controlling the trajectories of self-written waveguides in photopolymer," *J. Opt. Soc. Am. B* **35**, 2046 (2018).
28. N. Hô, B. Bourliaguet, J. M. Laniel, R. Vallée, and A. Villeneuve, "Observation of filamentation in As₂S₃," in *Nonlinear Guided Waves and Their Applications* (OSA, 2001), p. WC8.
29. J. Toombs, M. Luitz, C. Cook, S. Jenne, C. C. Li, B. Rapp, F. Kotz-Helmer, and H. Taylor, "Volumetric Additive Manufacturing of Silica Glass with Microscale Computed Axial Lithography," arXiv:2110.01651 [physics] (2021).
30. C. Chung Li, J. Toombs, and H. Taylor, "Tomographic color Schlieren refractive index mapping for computed axial lithography," in *Symposium on Computational Fabrication, SCF '20* (Association for Computing Machinery, 2020), pp. 1–7.
31. C. M. Rackson, K. M. Champley, J. T. Toombs, E. J. Fong, V. Bansal, H. K. Taylor, M. Shusteff, and R. R. McLeod, "Object-space optimization of tomographic reconstructions for additive manufacturing," *Additive Manufacturing* **48**, 102367 (2021).
32. Y. Jian, Y. He, L. Zhao, A. Kowalczyk, W. Yang, and J. Nie, "Effect of Monomer Structure on Real-Time UV-Curing Shrinkage Studied by a Laser Scanning Approach," *Advances in Polymer Technology* **32**, (2013).
33. D. L. Kurdikar and N. A. Peppas, "The volume shrinkage, thermal and sorption behaviour of polydiacrylates," *Polymer* **36**, 2249–2255 (1995).